A Wind Tunnel Inlet Flow Simulation

Upender K. Kaul*
NASA Ames Research Center
Moffett Field, California

Introduction

THE flow into an open-return wind tunnel inlet is simulated using the Euler equations. The calculation is time accurate and is performed to achieve a steady-state solution. The present approach affords a potential to simulate inlet treatment effects such as those caused by vanes and screens; the atmospheric boundary layer and the wind shear can be simulated by prescribing a total pressure gradient and the changing velocity vector, respectively, through the inflow boundary condition. The predictions are in reasonable agreement with the experimental data. The present investigation is a part of an effort to improve the test section flow quality of the open-return wind tunnel of the National Full-Scale Aerodynamics Complex (NFAC) by numerically analyzing the aerodynamics of the 80×120 inlet.

Method

The inlet flow is simulated by solving the unsteady compressible Euler equations in three dimensions using MacCormack's explicit predictor-corrector scheme[1,2] in Cartesian coordinates with a finite volume formulation. The Euler code used here is a modified version[3] of that used in Ref. 4. The code was used to simulate the flow induced in the wind tunnel by a fan downstream of the test section (sink-type flow).

The three-dimensional computational grid for the inlet, as shown in Fig. 1, is divided into two zones. The grid is generated algebraically and plane by plane using an interpolation scheme. The grid size for zone 1 is $11 \times 32 \times 30$ and for zone 2 is $39 \times 19 \times 17$. The nozzle has a 5:1 contraction ratio, defined from where the inlet cowl ends (the $x = 0$ cross-flow plane) to the test section. A planar grid, enlarged near the cowl and representing a horizontal cut (i.e., the z plane), is shown in Fig. 2. The computations are carried out corresponding to quiescent atmospheric conditions at the upstream boundary. Initially, stagnation conditions are imposed everywhere. The pressure drop that generates the flow in the inlet and yields a given test section velocity is introduced at the downstream boundary gradually in time. The flow can be imagined to exit at the downstream boundary at somewhat lower than the upstream stagnation pressure. This pressure is given by

$$p_e = p_s - \tfrac{1}{2}\rho q_e^2$$

in the steady incompressible limit, where the subscripts e and s refer to the exit and stagnation conditions, respectively, and q is essentially the horizontal velocity at the exit.

The implementation of the solid boundary condition at the convex corners (e.g., B in Fig. 2) is done in such a way that the same image (dummy) volume element is used to satisfy the boundary conditions (corresponding to surface tangency) at the two interior nodes adjacent to the corner. This is done sequentially in the three coordinate directions as the fluxes are accumulated in the integration process, thereby removing the corner discontinuity. Around the regions such as the external cowl, where the curvature is relatively large, the pressure at the image node next to the wall is found from the conservation of momentum normal to the cowl surface. This reduces to a balance between the centrifugal force and the pressure gradient in that direction.[5] This condition is given by

$$\partial_n p = \rho V^2 / r$$

where n is the direction normal to the surface, V is the tangential velocity at the curved surface, and r is the radius of curvature of the surface.

At the downstream boundary, a nonreflecting boundary condition for the pressure[6] was used, while the other four in-

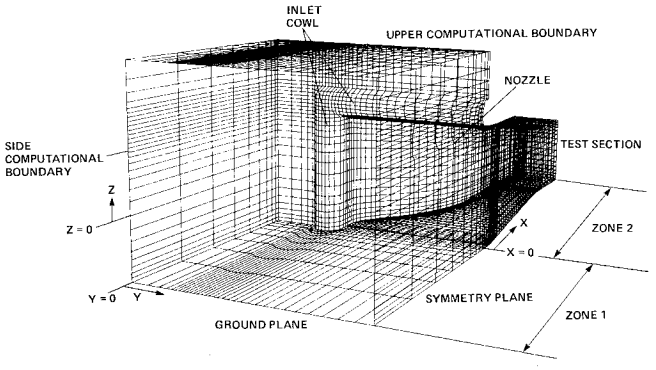

Fig. 1 Perspective view of the inlet model of the NFAC open-return wind tunnel, looking at the symmetry plane and into the tunnel inlet.

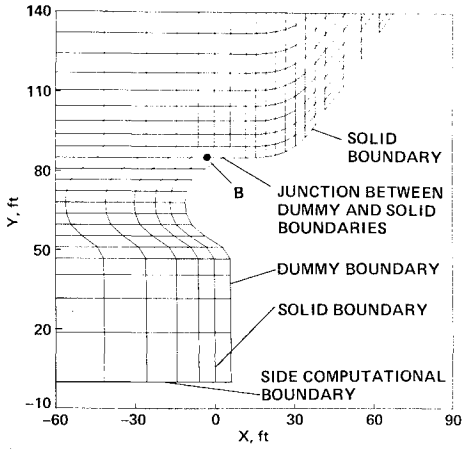

Fig. 2 Planar grid in the z plane enlarged near the inlet cowl.

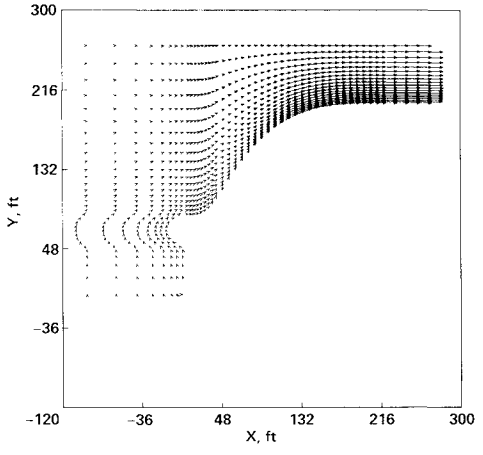

Fig. 3 Vector plot showing general behavior of the flow.

Received Dec. 4, 1984; presented as Paper 85-0437 at the AIAA 23rd Aerospace Sciences Meeting, Reno, NV, Jan. 14-17, 1985; Technical Note received July 1, 1985. This paper is declared a work of the U.S. Government and therefore is in the public domain.

*Principal Analyst, Informatics General Corporation, Palo Alto, CA. Member AIAA.

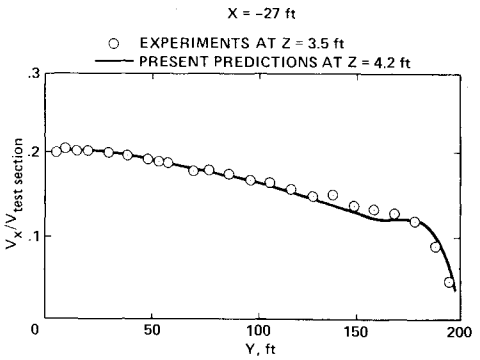

Fig. 4 Normalized axial velocity variation with the spanwise distance y.

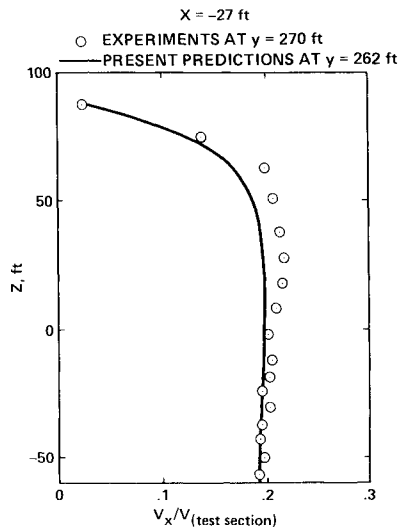

Fig. 5 Normalized axial velocity variation with the height z.

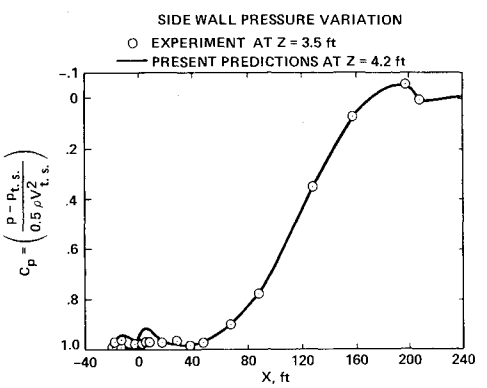

Fig. 6 Pressure variation on the side wall centerline with downstream distance x.

dependent variables were simply extrapolated. The boundary condition on pressure is given by

$$\partial_t p - \rho c \partial_t u + \alpha(p - p_e) = 0$$

where α is an empirical parameter that determines the rate at which the transients die out before steady state is attained.[6]

Results

Computations were carried out at the test section Mach number, $M = 0.15$. The results from the computations are shown in Figs. 3-6. The converged results correspond to a relative convergence criterion on pressure such that

$$|(p^{m+1} - p^m)/p^m| < 0.0001$$

over the entire flowfield, where m is the time-step index. Convergence to a steady state took about 5000 time steps (400 CPU seconds on Cray-XMP/22). The velocity vector plot in the $x-y$ plane, as shown in Fig. 3, indicates qualitatively the behavior of the inlet flow. Figure 4 shows a variation of the axial velocity normalized by the test section velocity with the spanwise coordinate y at an x station situated 27 ft upstream of the inlet and close to the $z = 0$ plane. The agreement with the experimental data in this case is quite good. Figure 5 shows a variation of the normalized axial velocity with the vertical coordinate z at $x = -27$ ft near the symmetry plane between the two side walls of the tunnel. The predictions are again in good agreement with the experimental data. Pressure variation with the downstream distance (i.e., C_p distribution) near the side-wall centerline (the plane $z = 0$) is shown in Fig. 6. The comparison between the computational results and the experimental data is excellent, except in the region of the separation bubble (seen experimentally) for which the pressures are slightly overpredicted relative to the experiment. The present predictions and the panel method predictions are also seen to be in good agreement inside the inlet.

Conclusions

A three-dimensional external-cum-internal flow through an open-return inlet has been successfully simulated using the Euler equations; the pressures and the velocity profiles inside the inlet of the NFAC have been predicted. The predictions are in good agreement with the experimental data.

Acknowledgment

The author thanks Dr. J.M. van Aken of the University of Kansas Center for Research, Inc. and Mr. M.S. Reinath of NASA Ames Research Center for having graciously provided the experimental data.

The panel method predictions were made by Mr. James C. Ross of the NASA Ames Research Center.

References

[1]MacCormack, R.W., "The Effect of Viscosity in Hypervelocity Impact Cratering," AIAA Paper 69-354, 1969.

[2]MacCormack, R.W. and Paullay, A.J., "Computational Efficiency Achieved by Time Splitting of Finite Difference Operators," AIAA Paper 72-154, 1972.

[3]Kaul, U.K., Ross, J.C., and Jacocks, J.L., "A Numerical Simulation of the NFAC (National Full-Scale Aerodynamics Complex) Open-Return Wind Tunnel Inlet Flow," AIAA Paper 85-0437, Jan. 1985.

[4]Jacocks, J.L. and Kneile, K.R., "Computation of Three-Dimensional Time-Dependent Flow Using the Euler Equations," AEDC-TR-80-49, 1981.

[5]Eidelman, S., Colella, P., and Shreeve, R.P., "Application of the Godunov Method and Higher order Extensions of the Godunov Method to Cascade Flow Modelling," AIAA Paper 83-1941, 1983.

[6]Rudy, D. and Strikwerda, J., "A Non-Reflecting Outflow Boundary Condition For Subsonic Navier-Stokes Calculations," *Journal of Computational Physics*, Vol. 36, 1980, pp. 55-70; also NASA ICASE Rept. 79-2, 1979.